A Study of Soft and Hard Impact Effects in Single-Particle Impact Dampers

Muhammad Ayaz AKBAR[1,3], Waion WONG[1*], Emiliano RUSTIGHI[2]

[1] Department of Mechanical Engineering, The Hong Kong Polytechnic University, Hong Kong SAR

[2] Department of Industrial Engineering, University of Trento, Italy

[3] Institute of Advanced Interdisciplinary Technology, Shenzhen MSU-BIT University, Shenzhen 518172, China

Abstract

Single-particle impact dampers (SPIDs) are simple, yet impactful devices that mitigate vibrations in various applications such as high-rise structures, machinery, and satellites. However, the high-intensity impact forces transmitted to the host structure pose a risk to older and vulnerable structures. Therefore, this study investigates the performance of SPIDs with soft impacts, employing viscoelastic materials to minimize the impact forces and noise levels without degrading the damping performance. Four different materials (rubber, ethylene-vinyl acetate, acrylic and poly-urethane foams) exhibiting different viscoelastic properties are studied and compared with hard impact. An approximate Voigt model for the stiffness and damping coefficient of viscoelastic material is used to conduct numerical simulations and to evaluate the damping performance of SPIDs. Dynamic mechanical analyser (DMA) tests are conducted to determine the dynamic properties of viscoelastic materials. An experimental rig which includes a single-degree-of-freedom host structure, and a prototype SPID is designed and manufactured. Experiments are conducted to determine the damping performance, impact force and noise level with soft impacts and the results are compared with hard impacts. The results reveal a 40% reduction in vibration amplitude at resonance frequency, an impressive 96% reduction in impact force at resonance, an 11.55dB reduction in the noise level using poly-urethane foam (softest impact) compared to steel (hard impact). Although viscoelastic materials may not be suitable in harsh environmental conditions, this study demonstrates that introducing a viscoelastic material in SPID can resolve its major drawbacks such as impact forces and noise leading to a simple, cost-effective, and safe SPID.

Keywords: Single-particle impact damper (SPID); Passive vibration control; Viscoelastic materials; Structural integrity

1. Introduction

Damping is a crucial element in engineering applications, especially focusing on vibration control and noise reduction (Housner et al., 1997). Passive vibration control technologies (Djemal et al., 2019; Meador and Mead, 1999) gained further importance due to their ability to operate without external power, including the use of particle impact dampers (Gagnon et al., 2019). Passive dampers, despite their advantages, face several design, installation, and performance constraints. For instance, viscous dampers can suffer from oil leakage, increased weight, and complex tuning and installation processes (Nehemy et al., 2023; Koutsoloukas et al., 2022; Jaisee et al., 2021; Enríquez-Zárate et al., 2019; Salvi et al., 2018; Trindade, 2016). Tuned Mass Dampers (TMDs) also operate effectively only within a narrow range of design parameters. These challenges have prompted other engineering disciplines to seek solutions to these costly design requirements. Recent advancements in materials and engineering techniques have mitigated some of these concerns, leading to the successful use of TMDs in civil and structural applications (Wang et al., 2023; Jami et al., 2024; Rupakhety et al., 2020; Li et al., 2021b; Li et al., 2021a; Gao et al., 2020; Banerjee et al., 2022; Araz, 2022). However, the high cost of designing and implementing passive dampers continues to drive researchers to explore simpler alternative solutions to address these challenges. Therefore, particle impact dampers have gained significant attention due to their simplicity, effectiveness, and flexibility in a wide range of industrial applications (Xia et al., 2011; Els, 2011; Bai et al., 2009; Sims et al., 2005; Simonian, 2004). By introducing moving particles, these dampers can dissipate energy and reduce vibration amplitude, leading to improved performance and enhanced structural integrity. However, these dampers exhibit highly nonlinear phenomena during operation (Wong and Rongong, 2009). Nonlinearity generates a huge challenge to develop theoretical models for their optimal designs (Gagnon et al., 2019; Lu et al., 2018) and, there is still a lack of analytical models to estimate the response of a primary structure with particle impact damper.

In recent research, there has been a growing focus on Single-Particle Impact Dampers (SPIDs) due to their relatively simpler analysis and easier design methodology, which consist of a single moving mass in a cavity installed onto the primary structure (Wang et al., 2022; Zhang et al., 2022; Żurawski et al., 2023; Akbar et al., 2023; Akbar and Wong, 2023). The operation of SPIDs is based on the principles of momentum exchange and energy dissipation through impacts. The single mass oscillates in response to the structural vibrations and collides with the primary structure within the cavity, each collision results in momentum exchange and energy dissipation depending on the nature of the impact and mass ratio (Masri, 1970).

Through the study of SPIDs, valuable insights can be gained regarding the design and optimization of impact dampers. However, most previous research has mainly focused on hard impacts (Prasad et al., 2022; Meyer and Seifried, 2020; Huang et al., 2021; Yang and Wang, 2019; Snoun and Trigui, 2018). In literature, most of the numerical studies model a SPID for simplicity in the analysis (Wang and Dan, 2022; Wei-ming et al., 2019; Huang et al., 2020; Trigui et al., 2009; Lu et al., 2011) as it can be extremely difficult to predict the dynamic response of the system with numerous moving particles (Masri, 1970; Wong and Rongong, 2009). SPID is the simplest type of impact damper which can be designed and installed easily on any structure (Zhang et al., 2022; Wang and Dan, 2022; Safaeifar and Sheikhi Azqandi, 2021). The impacts are usually modelled with a coefficient of restitution and the contact between colliding bodies is not considered. SPID with hard impacts, thanks to large coefficients of restitution and momentum exchanges, still provides reasonable damping to the primary structure. However, during operation they may compromise the structural integrity and increase the noise levels. These drawbacks pose significant challenges, limiting the practical applications of SPID technology. The iterative impact force generated by heavier single particle on the primary structure may lead to damage or failure especially in vulnerable and old structure. On the other hand, a soft impact obtained by introducing a viscoelastic buffer might result in larger energy dissipation due to material deformation but also in a lower momentum exchange. This dissipation of energy leads to a reduction in the overall system response, effectively attenuating vibrations and mitigating structural resonance. Experimental studies on buffered particles impact dampers have been carried out (Lu et al., 2012; Wang et al., 2020) where several types of impact surfaces and particles were studied. It was shown that collision hardness is negatively correlated to the reduction of the host structure accelerations. However, the use of soft impact in SPIDs still draw contrasting views and the impact forces on the host structure were not previously examined.

This study investigates the damping effects of soft and hard impacts in a SPID for the first time. In particular the fundamental design objective is to find a solution that minimizes the high impact forces and noise levels arising from SPIDs without compromising the damping performance (Żurawski et al., 2023). Soft impact involves the use of viscoelastic materials that can deform and dissipate energy during an impact, whereas a hard impact refers to rigid materials that exhibit minimal deformation. Understanding the influence of impact materials on the performance of single-mass dampers is of utmost importance. The choice of impact material directly affects the system's ability to absorb energy, dissipate vibrations, and reduce noise levels. The overall hypothesis is that SPID with soft impacts can provide better damping efficiency than SPID with hard impact and protect the primary structure from impact forces generated by iterative impacts with minimal noise generation.

To analyse the problem, a numerical model with consideration of the viscoelastic behaviour of the impact materials is constructed. The Voigt model is used to approximate the stiffness and damping coefficient of viscoelastic material for time-history simulations. A comprehensive analysis using a numerical model is performed for the optimal design of the SPID. In addition, an experimental rig is designed and built to validate the conclusions drawn from the numerical model. Various viscoelastic materials (rubber, acrylic foam, Ethylene vinyl acetate (EVA) plastic, Polyurethane (PU) foam) are used in the experiments to study the damping performance of SPIDs. Dynamic mechanical analyser (DMA) compression tests are performed to determine the dynamic properties of viscoelastic materials such as loss modulus, storage modulus and loss factor. Furthermore, the damping performance of a SPID with viscoelastic impact surfaces is compared with rigid metallic impact surfaces in the damper cavity determined from experiments. During the experimental tests both impact forces and emitted noise have been recorded.

Overall, this study provides a solution to the problems associated with the existing design of SPID with hard impact. SPID with hard impact generates iterative impact forces and excessive noise during operation leading to compromising structural integrity and comfort of living. SPID with soft impact is introduced and studied to enhance the damping efficiency and protect the primary structure from impact forces and excessive noise levels during operation. On the other hand, viscoelastic impact materials may limit the applications of SPID. Mechanical properties of viscoelastic materials are dependent on several factors, including temperature, frequency of vibration and force amplitude. Nonetheless this work might open the road to future studies on the effect of temperature or environment on the damping performance of viscoelastic impact materials.

2. Methodology

In this section, the methodology for the numerical and experimental methods is described. The theoretical model is developed and discussed with numerical analysis.

2.1. Numerical model

The SPID consists of a single mass placed in a cavity within the primary structure often free to move in one direction. Often, a multiparticle impact damper is also designed as a SPID for simpler analysis in theory.

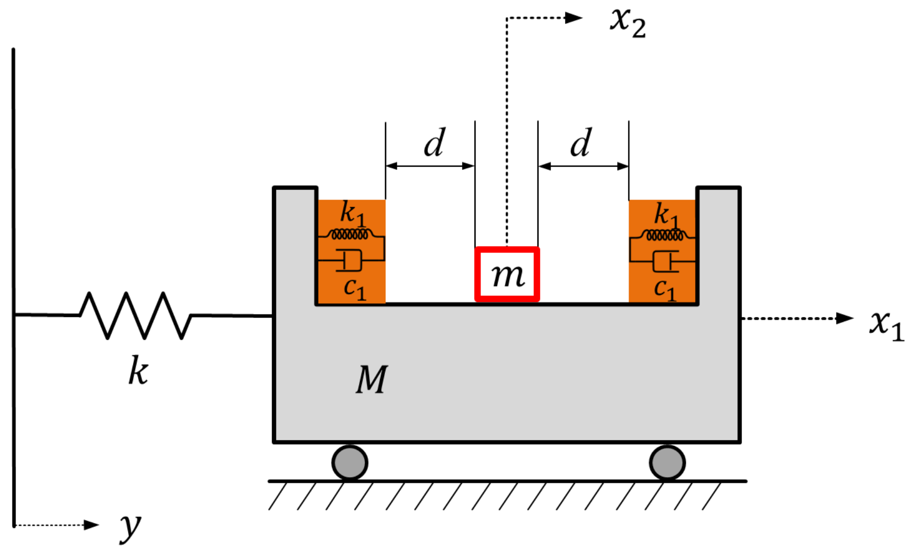

Figure 1. Mechanical model of a SPID with viscoelastic material attached to an SDOF system represented by the Voigt model.

A mechanical model of a SPID with viscoelastic material attached to an SDOF structure is presented in Figure 1. Here M is the mass, k is the stiffness, and x_1 is the displacement of the primary structure. While m is the mass, x_2 is the displacement of the particle. The clearance magnitude between particle and primary mass is represented by d, and y is the base motion. The particle collides with the primary structure when $(x_1 - x_2 = d)$. Furthermore, the stiffness of the viscoelastic material can be described by complex stiffness as (Wong et al., 2018),

$$k_s(\omega) = \nu E_c(\omega) = \nu\big(E_s(\omega) + \mathrm{j}E_l(\omega)\big) = \nu E_s(\omega)\big(1 + \mathrm{j}\eta(\omega)\big) \tag{1}$$

In the above equation, ω is the frequency, ν is the shape factor related to the geometry of the viscoelastic material, and $E_c(\omega)$ is the complex elastic modulus of the viscoelastic material. $E_s(\omega)$ and $E_l(\omega)$ are the storage modulus and loss modulus, respectively, of the viscoelastic material. $\eta(\omega)$ is the loss factor defined as (Wong et al., 2018),

$$\eta(\omega) = \frac{E_l(\omega)}{E_s(\omega)} \tag{2}$$

The mechanical properties of viscoelastic materials can be nonlinear due to the dependence on various parameters. The complex shear modulus depends on the vibration frequency and the temperature of the material. In this study, the temperature effect on the viscoelastic material is assumed constant in time. The moduli of the viscoelastic material in this study are therefore shown as functions of the vibration frequency only.

The equation of motion of the primary mass and particle shown in Figure 1, when the particle is not in contact with the viscoelastic material can be written as,

$$M\ddot{x}_1 + k(x_1 - y) = 0 \tag{3}$$

$$m\ddot{x}_2 = 0 \tag{4}$$

When the particle is in contact with the viscoelastic material, the equations of motion of the primary structure and particle can be written as,

$$M\ddot{x}_1 + k(x_1 - y) + \mathrm{F_c} = 0 \tag{5}$$

$$m\ddot{x}_2 - \mathrm{F_c} = 0 \tag{6}$$

F_c in Equations (5) and (6) is a nonlinear contact force. Generally, impact force depends on the properties of the impact surface, relative position, and velocity between colliding bodies. The hysteretic damping model with complex stiffness is acausal, although it describes the material appropriately in the frequency domain but cannot be used for time domain simulations, hence an approximate model is required for time domain simulations.

Friction between the primary mass and particle is another parameter which can influence the motion of the particle. However, it has been verified that the large amount of friction has a negative effect on the damping performance of SPID (Akbar et al., 2024). Therefore, the friction effects are ignored in the numerical analysis for further simplification.

The behaviour of viscoelastic material can be overly complicated and its dependence on vibration frequency makes it difficult to model accurately. Therefore, an approximation is needed for numerical analysis. In this study, the Voigt model, which is a linear representation of viscoelastic behaviour, is used to approximate the stiffness and damping component of the viscoelastic material from the complex modulus. Voigt model is commonly used due to its simplicity and direct approach in modelling viscous and elastic behaviours of any viscoelastic material. It consists of a spring element and a dashpot element connected in parallel as shown in Figure 1. The spring element represents the material's elastic response, generating a force proportional to the displacement. The dashpot element represents the material's viscous response, generating a force proportional to the velocity. The Voigt model provides a simplified representation of viscoelastic behaviour which is frequency independent and is commonly utilized in engineering and materials science to analyse and predict the response of viscoelastic materials under different loading conditions.

The viscoelastic force from the Voigt model (Zhou et al., 2016) can be determined as,

$$F_c = k_1 H(x_1, x_2) + c_1 \mathrm{G}(\dot{x}_1, \dot{x}_2) \tag{7}$$

Here k_1 represents the elastic behaviour or the stiffness of the viscoelastic material. It can be related to the storage modulus of the viscoelastic material as $k_1 = \nu E_s(\omega)$, which is the real part of the complex modulus. On the other hand, c_1 represents the viscous behaviour of the viscoelastic material or the damping and can be related to the loss factor and vibration frequency (f) as $c_1 = \nu E_s(\omega)\eta/f = k_1\eta/f$, which is the imaginary part of the complex modulus (Kaul, 2021; Li, 2020; Momani et al., 2021). Utilizing the approximate model to represent the viscoelasticity of impact material, it is possible to analyse the system numerically. $H(x_1, x_2)$ and $\mathrm{G}(\dot{x}_1, \dot{x}_2)$ are functions representing the relative positions and velocity between primary structure and particle (Masri and Caughey, 1966; Chatterjee et al., 1995). These functions are defined as,

$$H(x_1, x_2) = (x_1 - x_2 - d)\, U(x_1 - x_2 - d) + (x_1 - x_2 + d)\, U(-x_1 + x_2 - d) \tag{8}$$

$$\mathrm{G}(\dot{x}_1, \dot{x}_2) = (\dot{x}_1 - \dot{x}_2) U(x_1 - x_2 - d) + (\dot{x}_1 - \dot{x}_2) U(-x_1 + x_2 - d) \tag{9}$$

$U(x)$ is a unit-step function known as the "Heavyside" function in MATLAB software. The output of this function is 0 or 1. The step function detects the impact on either side of the boundary during numerical simulations. Furthermore, the natural frequency of the primary structure is defined as,

$$\omega_1 = \sqrt{\frac{k}{M}} \tag{10}$$

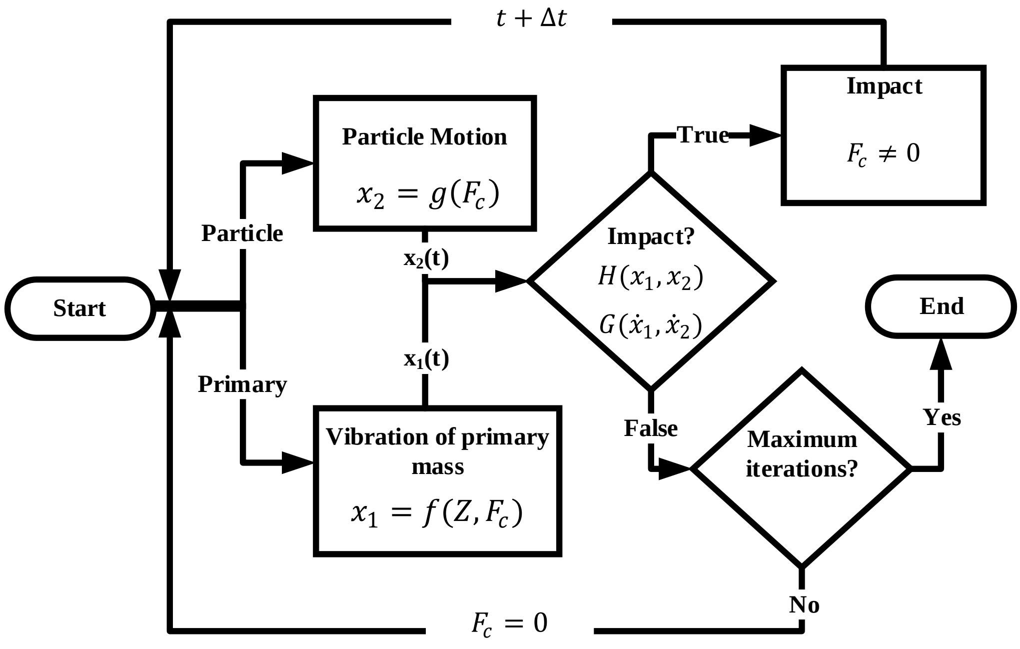

Figure 2. Flowchart of computation process.

A MATLAB program is written to simulate the system using the equations mentioned before. The flowchart of the computation process is presented in Figure 3. The primary structure vibrates under the influence of ground motion. The motion of particle starts with the impact. The computation algorithm keeps track of the positions of the primary structure and particle, an impact is detected whenever the positions of the primary structure x_1 and particle x_2 satisfy the impact conditions presented in Equations (8) and (9). When the impact is detected on either side of the cavity boundary, the impact force F_c is calculated based on the $H(x_1, x_2)$ and $G(\dot{x}_1, \dot{x}_2)$ and properties of the viscoelastic material $(k_1 - c_1)$. Now, the impact force is updated, and the equations of motion are computed again for the next time step under the influence of impact force. Time step in the numerical model is extremely important. A large time step will lose important information while a very small-time step may cost a huge computation power. Therefore, a trial-and-error base convergence analysis is performed to determine the appropriate time-step for displacement response of the system. The convergence analysis showed that the time step beyond 0.0001 sec leads to similar results up to 4 decimal places.

2.2. Experiment setup.

The experimental rig is comprised of a steel frame with dimensions measuring 600x200x100 mm. The base is fixed on a moving plate which is connected to a shaker. There are two laser displacement sensors (Panasonic HG-C1200) measuring the displacement of the top of the primary structure and the displacement of the base. The sketch of the experiment setup is shown in Figure 3a.

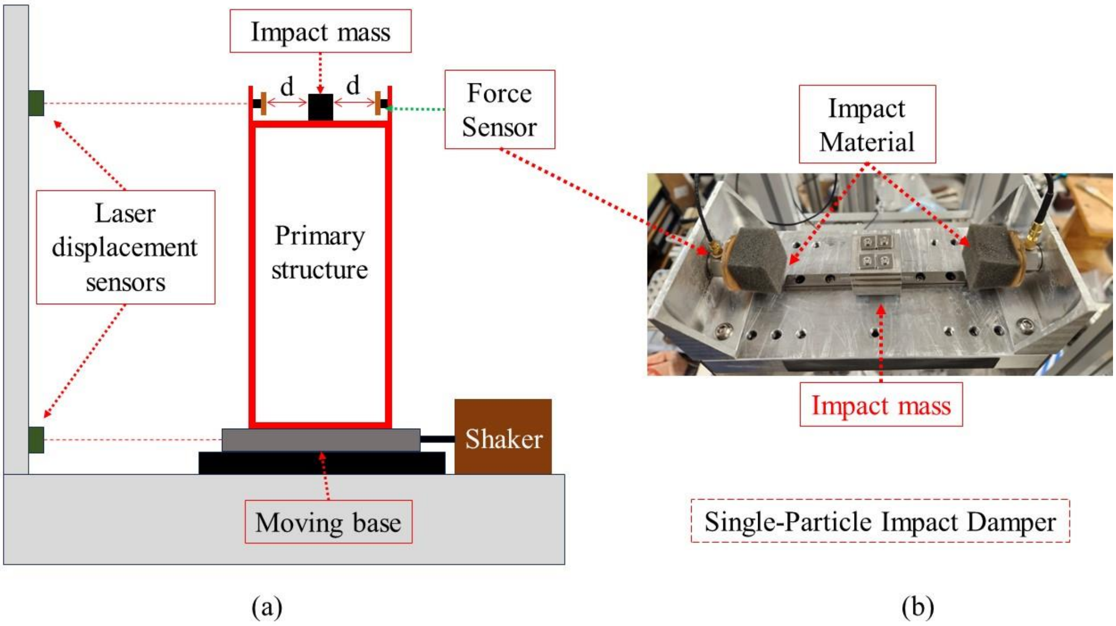

Figure 3. (a) Sketch of the experiment setup. (b) Developed SPID used in experiments

A SPID is designed and manufactured as shown in Figure 3b. A linear slider is installed on the top surface of the primary structure, and a sliding rail carrying the secondary mass can slide on it. The mass of the particle can be changed by choosing the number of plates fixed on the sliding part. The sliding mechanism ensures the movement of impact mass in one direction and minimizes the friction between primary and secondary mass. Moreover, Impact materials are installed on either side of the boundary. Two force sensors (B&K Delta Tron Type-8200) are installed to either end between the boundary and impact material. The force sensors record the impact force anytime sliding mass impacts with the impact material. Various impact materials are used in this study such as viscoelastic materials and rigid impact materials. Furthermore, clearance d is the distance between the particle and the primary structure wall. The clearance magnitude can be changed by moving the L-beams as shown in Figure 3b.

Free vibration tests are carried out to determine the parameters of the primary structure. The primary structure is provided with an initial displacement with no additional damper added to it. The free vibration response is recorded and the system parameters such as natural frequency and damping ratio are calculated by FFT and logarithmic decrement methods, respectively. Parameters of the primary structure are presented in Table 1.

Table 1. Calculated parameters of the primary structure

Parameter	Magnitude
Mass (M)	1.6 Kg
Natural Frequency (ω_1)	2.7 Hz
Damping ratio (ζ)	0.0038

2.3. Materials

In this section, the materials tested in this study are discussed. To see the effect of viscoelastic materials on the damping performance of the SPID, a few soft materials exhibiting viscoelastic properties are used and compared with the hard impact where no material deformation is evident. Viscoelastic materials are generally commercially available and have various applications in vibration control (Oyadiji, 1996). However, their mechanical properties such as elastic and viscous behaviour are not independent and cannot be selected separately. Their properties are usually dependent on the shape, material, and internal design. They exhibit nonlinear elastic and viscous behaviour generally dependent on the temperature and vibration frequency.

The materials used in this study are presented in Figure 4. Rubber, EVA rubber (obtained from a commercial anti-vibration pad), acrylic and PU foams exhibit viscoelastic properties and generate soft impacts. On the other hand, steel is used to produce hard impact. The hard impact is achieved by removing the viscoelastic materials from the walls of cavity, so that the particle mass hits the metallic walls, and the length of cavity is kept constant for every material. In general, the mechanical properties of viscoelastic materials are dependent on the vibration frequency and temperature. However, the effect of temperature is assumed to be constant and therefore, the properties are determined in the frequency domain only. The viscoelastic properties (storage modulus E_s, loss modulus E_l, loss factor η) are determined by performing dynamic mechanical tests through a dynamic mechanical analyzer (DMA- Mettler Toledo DMA1).

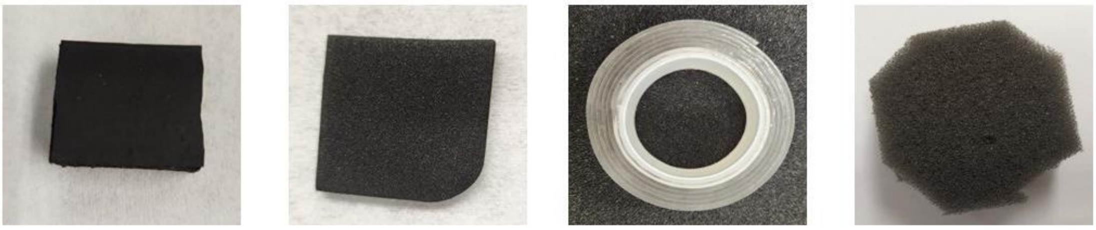

Rubber | EVA anti-vibration pad | Acrylic Foam | Polyurethane (PU) foam

Figure 4. Pictures of the viscoelastic materials used in this study.

The dynamic tests display the viscoelastic properties of the materials, as shown in Figure 5. Storage modulus, loss modulus, and loss factor are measured through DMA tests in the frequency domain at room temperature (approximately 25°C). Storage modulus is referred to as the elastic response of the material while the loss modulus is the viscous response of the material over the frequency span (Henriques et al., 2020). The loss factor is the measure of material damping and is defined as the ratio of loss modulus and storage modulus. Figure 6 shows that PU foam has a lower magnitude of storage and loss modulus. On the other hand, acrylic foam exhibits a higher loss factor with larger storage (elastic) and loss (viscous) moduli.

The natural frequency of our primary structure is around 2.7Hz, which shows that the frequency of interest in this case will be below 5Hz. In addition, the change in the material properties in frequency domain is not very marked, especially at low frequency vibrations. Therefore, this system can become equivalent to a material with constant hysteretic damping, which is not frequency dependent. Hence Voigt model can approximate the material response linearly. The Voigt model (Figure 1) describes the elastic effect with storage modulus and shape factor ($k_1 = \nu E_s$) , while the viscous part is represented by elastic part and loss factor ($c_1 = \nu E_s \eta / f = k_1 \eta / f$). Here, the viscoelastic factors such as E_l and η are selected from Figure 5 according to the natural frequency of the system. Furthermore, the shape factor (sometimes called the geometry factor) may directly influence the response of the viscoelastic materials. As the name states, the shape factor depends on the geometry or shape of the viscoelastic material and it can be calculated as $\mathrm{v} = A/L$ for rectangular shape and $\mathrm{v} = \frac{\pi D^2}{4L}$ for cylindrical shape; Here L is the length, A is the cross-sectional area, and D is the diameter in the case of a round sample.

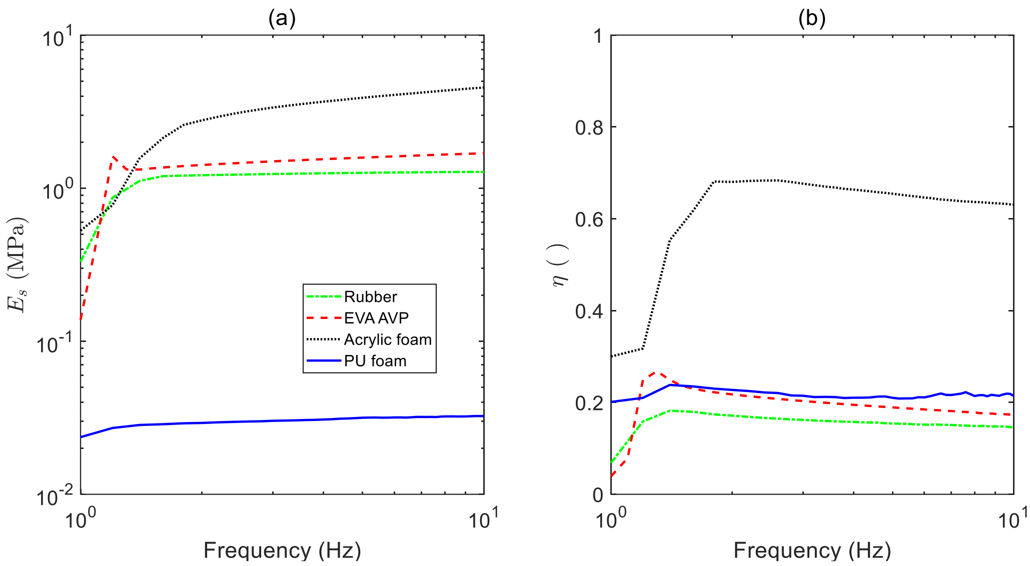

Figure 5. (a) Storage modulus E_s and (b) loss factor η obtained by performing dynamic mechanical tests for rubber, EVA anti-vibration pad, acrylic foam and PU foam materials.

3. Results and discussion

In this section, the results are presented for both numerical and experimental analysis. The key observations are discussed from the numerical results and are validated through experiments.

3.1. Model Validation

The results obtained in this study are obtained numerically and experimentally. It is well understood that the numerical model provides better understanding of any system behaviour over a wide range of parameters, as several combinations of the parameters can be tested. However, it is necessary to validate the numerical model for the accuracy of the results. Therefore, this section shows the direct comparison of the numerical and experimental results in time-domain. The Voigt model is a linear representation of the viscoelastic behaviour; therefore, a time-domain comparison can show the accuracy of the complete numerical model and if there are any discontinuities in time-domain. The cavity length is found to be the most important parameter in the SPID by various studies. Therefore, this validation is performed on three cavity lengths.

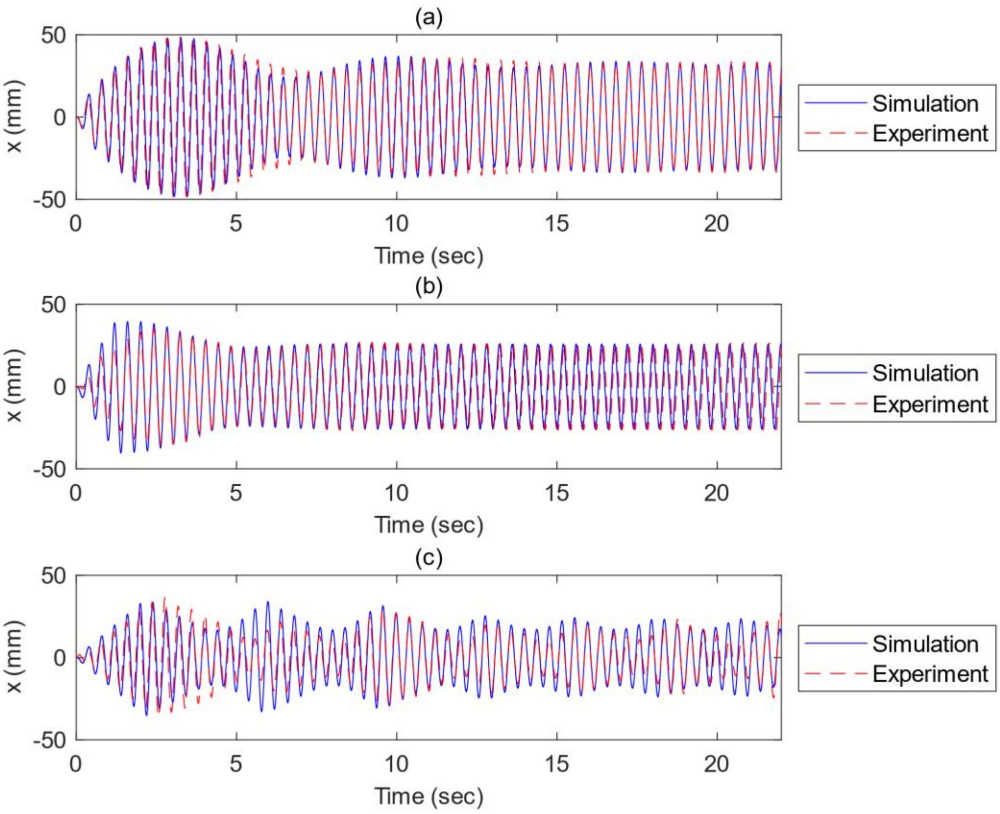

Figure 6. Comparison of experimental and numerical simulations results for PU foam.; (a) $\frac{d}{Y} = 5$; (b) $\frac{d}{Y} = 10$; (c) $\frac{d}{Y} = 15$

The comparison of numerical and experimental results over different magnitudes of relative clearance $\left(\frac{d}{Y}\right)$ is presented in Figure 6, where the relative clearance represents the cavity length (d) with respect to the base excitation magnitude (Y) for more generalized results. This comparison is for only PU foam which is the softest material among the other tested viscoelastic materials. The results show that the numerical model even with a linear representation of viscoelastic behaviour (Voigt model) provides good agreement with the experimental results. Considering the nonlinear characteristics of the whole system, the results show an overall good agreement between experimental and numerical approaches, specifically in Figure 6b. It has been observed that the clearance magnitude has a significant role in determining the nature of displacement and, the system responds with a steady state, a beating or a relatively chaotic behaviour depending on the clearance magnitude. An appropriate tuning of the clearance magnitude causes two impacts per cycle and a relatively steady state response. The appropriate choice of the clearance magnitude is the reason for the better agreement observed in Figure 6b.

3.2. Numerical Analysis

The theoretical model of a single-degree-of-freedom structure with a SPID is presented in Section 2.1. The model is simulated with the Runge-Kutta 4^{th}-order method. There are various important parameters that can affect the performance of a SPID such as viscoelastic properties, relative clearance, and mass ratio. It has been identified that the relationships of these design parameters are inter-linked, therefore, a contour map is used to observe the effect over several combinations.

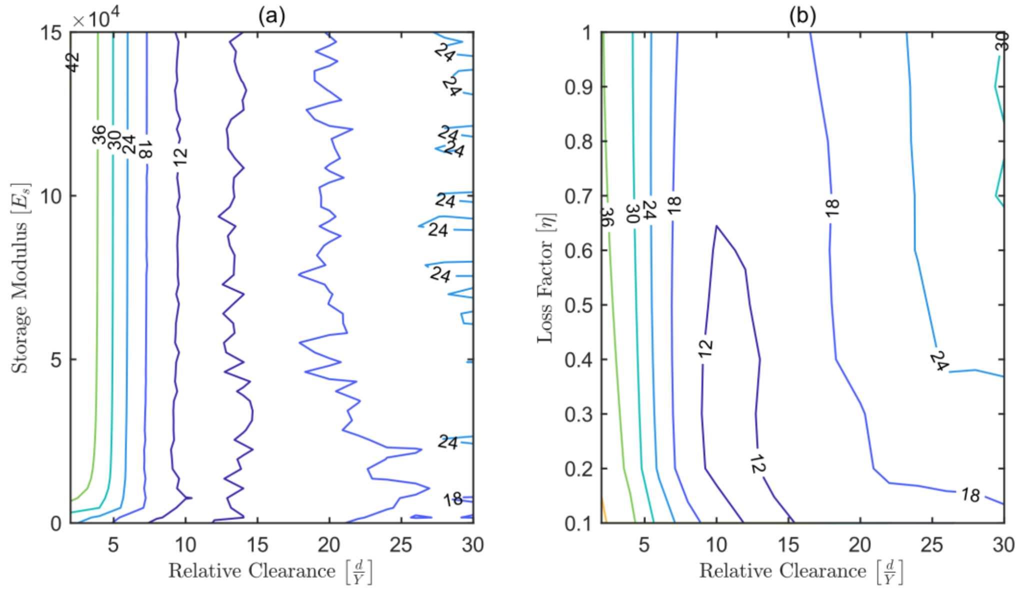

Figure 7. Contour of resonant vibration amplitude over various combinations of relative clearance $\left[\frac{d}{Y}\right]$ and, (a) stiffness νE_s with $\eta = 0.2$ or, (b) loss factor η with stiffness $\nu E_s = 1000$ N/m.

Figure 7 demonstrates how vibration amplitude changes across several combinations of important design parameters such as, relative clearance and properties of the viscoelastic materials. The contour of Figure 7a shows the resonant vibration amplitude over various combinations of relative clearance and storage modulus, while keeping the loss factor constant at 0.2. It can be observed from Figure 7 that the role of storage modulus of viscoelastic materials is minor in the damping performance of SPID. It is observed that the clearance magnitude is the critical parameter for the design of SPID. A similar conclusion can be gathered from Figure 7b which shows the contour map between several combinations of relative clearance and loss factor while keeping the stiffness $[\nu E_s]$ constant at 1000N/m.

As the influence of viscoelastic properties is minimal for the design of SPID, the impact force can be reduced with viscoelastic materials. Therefore, the impact force and noise produced during the operation of a SPID can be reduced by introducing a soft material at the walls of the container without degrading the damping performance. Three different relative clearances are tested with the soft materials illustrated in Section 2.3 and compared with a hard impact. The selected parameters of each viscoelastic material for numerical analysis are presented in Table 2.

Table 2. Viscoelastic properties selected for numerical simulations for soft impact.

Material	νE_s [kN/m]	Loss Factor (η)
Rubber	43.436	0.164
EVA anti-vibration pad	51.636	0.209
Acrylic Foam	112.43	0.683
PU Foam	1.0249	0.224

Steel does not show viscoelastic behaviour; however, it should have a very high stiffness and small viscous effect in comparison with the viscoelastic properties of these soft materials. The numerical model described for viscoelastic materials cannot represent the behaviour of steel, therefore, the damping performance of steel in the SPID for hard impact is only measured through experiments and compared with the soft impacts.

Figure 8 illustrates the vibration response of the structure with different clearance magnitudes and various viscoelastic materials. The numerical results indicate that the choice of material for soft impact has a minimal impact on the vibration response. PU foam has the lowest stiffness (storage modulus) among all the tested materials, resulting in enhanced energy dissipation and slightly improved damping performance. Interestingly, the vibration response remains relatively consistent across all tested materials.

Overall, it can be concluded that the choice of material for soft impact has less influence on the performance of a SPID. On the other hand, clearance magnitude is clearly the most influential and important design parameter for a SPID. The freedom in the choice of material in SPID allows for resolving other issues related to SPID in literature. High-intensity impact force and excessive noise are commonly mentioned problems associated with SPID. These problems can be resolved by employing a soft material (PU foam) at the walls of the cavity in SPID without compromising the damping performance. The softer material enhances the damping performance as well.

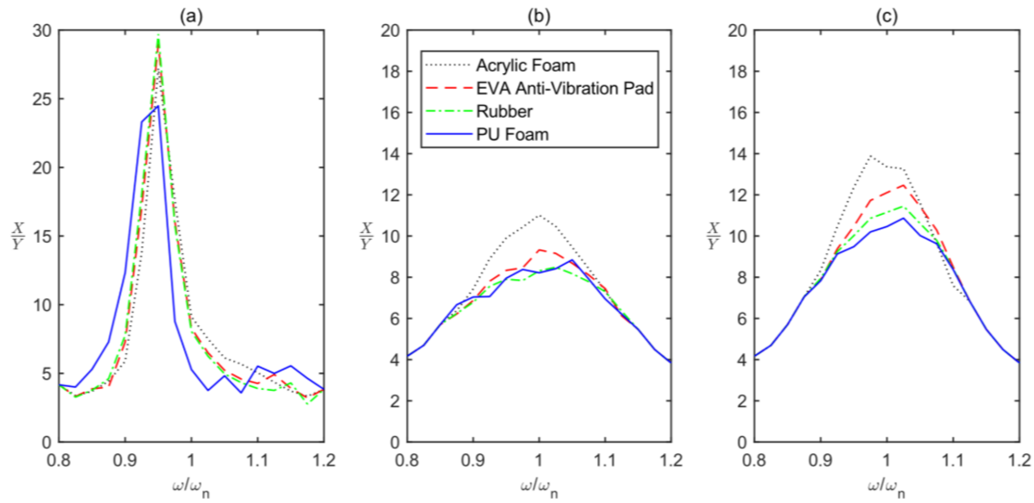

Figure 8. Simulated resonant transmissibility vibration amplitude at different clearance magnitudes with soft materials: (a) $d/Y = 5$; (b) $d/Y = 10$; (c) $d/Y = 15$.

3.3. Experimental validations

To further validate the conclusions from the numerical analysis, experiments are conducted on a single-degree-of-freedom structure with a SPID with different materials. The experimental setup is presented in Section 2.2.

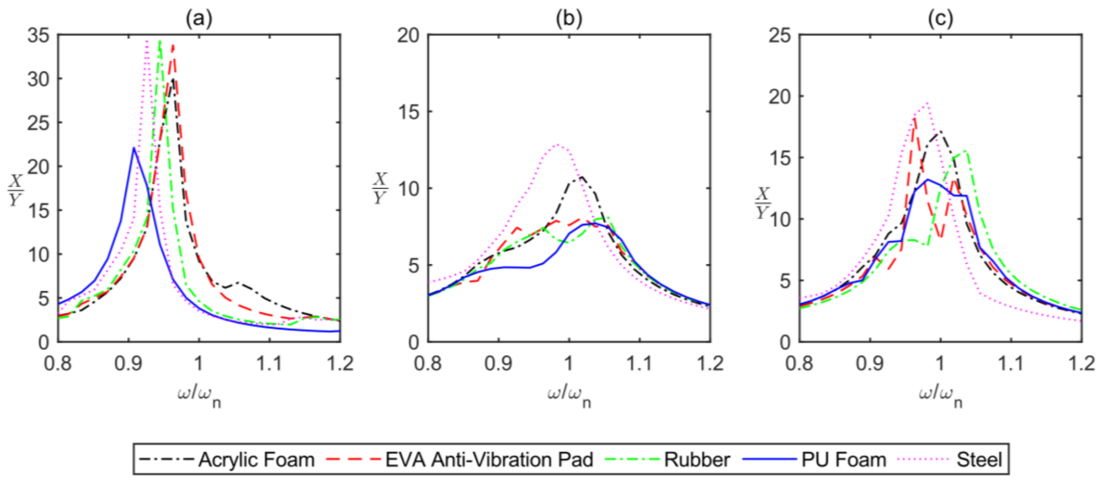

Figure 9. Resonant vibration amplitude recorded from experiments with soft and hard impact in SPID over different clearance magnitudes: (a) $d/Y \approx 5$; (b) $d/Y \approx 10$; (c) $d/Y \approx 15$.

Figure 9 shows the vibration amplitude of the primary structure with different clearance magnitudes. In the experimental analysis, a rigid material (steel) is tested alongside viscoelastic materials. The results show a similar trend found in the numerical analysis. It can be observed that there is a difference in damping performance with soft and hard impacts. The soft impacts (PU foam) in the SPID reduce vibration amplitude by 36%, 40% and 32% compared with hard impact (steel) for relative clearance of 5, 10, and 15, respectively. The damping mechanism of

SPID relies on the impacts and each impact results in momentum transfer and energy dissipation based on the material installed. A higher momentum transfer and lesser energy dissipation can be expected when a hard surface is used, and vice versa for a soft surface. The results here show that a soft impact enhances the damping performance of SPID and that the numerical difference between the viscoelastic materials under investigation is not significant. Hence, a balance of momentum transfer and energy dissipation is achieved with viscoelastic materials. For example, if a viscoelastic material is comparatively harder than other, a larger momentum transfer will occur and lesser energy dissipation. On the other hand, a larger energy dissipation and smaller momentum transfer is expected when a relatively softer material is installed. Overall, it seems that the balance of both phenomena is achieved leading to almost identical damping performance (Wang et al., 2020).

Table 3. Comparison of experimentally recorded and simulated vibration amplitude over different relative clearances of SPID

$\frac{d}{Y}$	Acrylic Foam		EVA anti-vibration pad		Rubber		PU Foam		Steel
	Exp.	Sim.	Exp.	Sim.	Exp.	Sim.	Exp.	Sim.	Exp.
5	30.16	27.19	33.84	28.99	34.52	29.70	22.11	24.48	34.52
10	10.73	11.01	8.09	9.32	8.09	8.41	7.71	8.84	12.87
15	17.15	13.88	18.46	12.46	15.60	11.45	13.21	10.86	19.41

These results support the initial hypothesis that a hard impact enhances the momentum exchange between the primary mass and the particle with minimal energy dissipation. In contrast, a softer impact achieves a balance between momentum exchange and energy dissipation through material deformation and internal complex structure. It becomes apparent that when a hard impact occurs between the primary structure and the particle, the impact force and noise during operation will be higher. Conversely, a softer impact leads to minimal noise, lower impact force, and better damping performance. Furthermore, the dimensionless vibration amplitude of SDOF structure is compared in Table 3 gathered from simulations and experimental data. The comparison shows that there is a good qualitative agreement between simulations and experimental data.

To verify the reduction in impact force exerted on primary structure, two force sensors are installed on either wall of the cavity in a SPID as shown in Figure 3b. The impact force data is recorded for each impact material and compared in Figure 10. As the resonance peak might shift slightly with different damper settings, the impact force is measured for the whole set of excitation frequencies. Maximum impact force for a specific setting of SPID is determined from the dataset. The results show that the maximum impact force exerted on the primary structure is reduced significantly by installing a viscoelastic material in SPID. The impact force is reduced by 96%, 97%, and 96% for relative clearance of 5, 10, and 15 respectively by using PU foam instead of rigid plastic. It shows that a soft impact absorbs the impact force due to material deformation and the internal structure of the viscoelastic materials. However, a rigid material such as steel transfers the impact force to the primary structure and repeated intense impact forces can be harmful to structures.

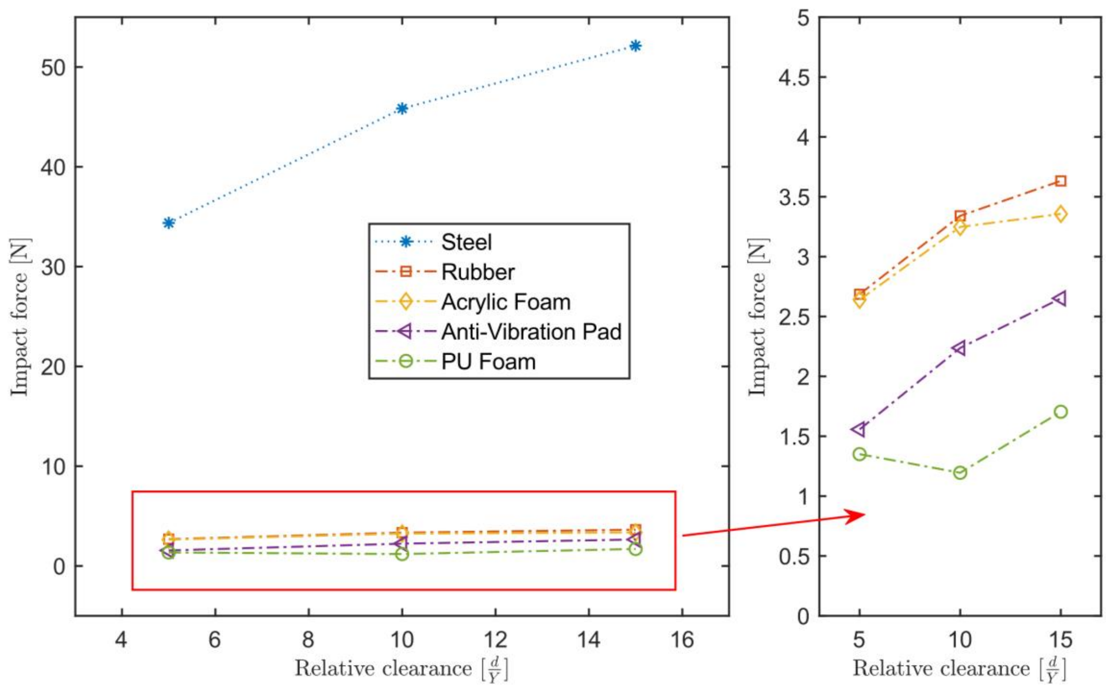

Figure 10. Impact force exerted on primary structure from SPID with different impact materials.

One of the key problems associated with SPID is the high noise levels during operation. Apparently when a metallic particle is colliding with a metallic surface of cavity in SPID, it generates continuous high intensity noise, and this continuous hitting noise is annoying to the living beings around. Since the objective of this study is to compare the soft against hard impact surfaces, we record noise levels of hard impact when no soft material is installed, and compare it to soft impact when PU foam, the softest material in this study, is used. To show the noise generated with the proposed SPID with soft impact, the noise during the experiments with soft and hard impact are recorded with a B&K free filed microphone (Type 4189). The audio data from microphone provides sound pressure levels in Pascal (Pa) units. This audio data is processed with a MATLAB Audio Toolbox to determine the sound pressure level (SPL) in decibel units at resonance. The results are presented in Figure 11, and the hard impact has peaks whenever there is an impact between particle and primary structure. The hard impact shows a maximum noise level of 80.88 dB, while the maximum noise level with soft impact is calculated as 69.33dB. The results show that a SPID with soft impact does not generate any significant noise to pollute the surroundings, while a SPID with hard impact can raise the noise levels by almost 11.55dB.

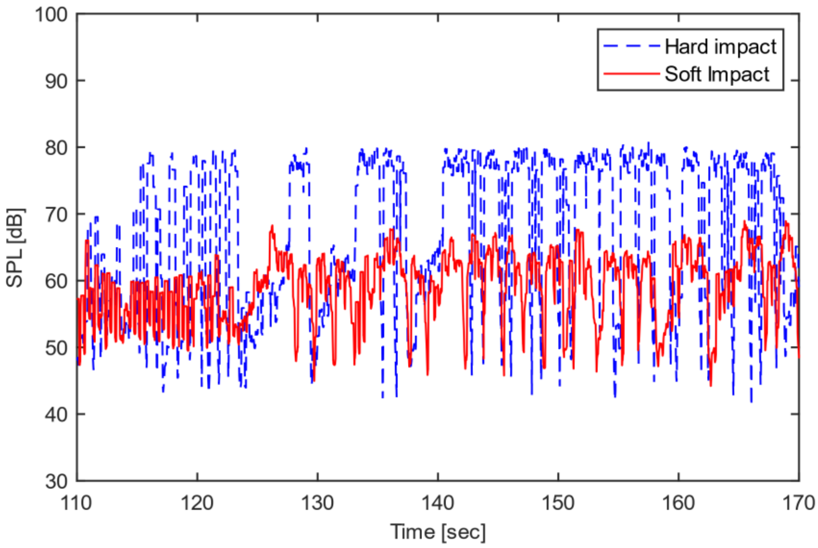

Figure 11. Recorded noise level [dB] during the operation of SPID at resonance with soft (PU foam) and hard impact (steel).

Overall, this study compares the traditional design of single-particle impact with hard impacts (metal-to-metal) with the proposed design of SPID with soft impacts (metal-to-viscoelastic). Four viscoelastic materials with different properties are tested and compared with steel as hard impact. PU foam was found to be the best performing viscoelastic material among the soft impact in this study. Therefore, maximum vibration amplitude, impact force, and noise level are compared for the PU foam and steel at best clearance magnitude found in this analysis, as shown in Table 4. It shows that the soft impact (PU foam) can enhance the performance of SPID in all departments, allowing a safe and sound design with simplest design and analysis procedure.

Table 4. Comparison of the performance of soft and hard impact in best performing case; $\left(\frac{d}{Y} \approx 10\right)$.

Parameter	Soft Impact [PU Foam]	Hard Impact [Steel]
Vibration amplitude $\left(\frac{X}{Y}\right)$	7.71	12.87
Impact Force	1.19N	45.84N
Noise level	69.33dB	80.88dB

4. Conclusions

SPID is relatively simpler to design and install compared to other types of particle impact dampers. Besides the various advantages, SPID has a few major challenges which directly influence the integrity of primary structure and surroundings. In conclusion, this study focused on addressing the challenges associated with the SPID by integrating soft-impact materials to mitigate larger impact forces and noise levels. The main findings of this research are:

1. The working principle of SPID is based on momentum transfer and energy dissipation through various impacts between primary structure and particle mass. Therefore, the nature of impact directly influences the momentum transfer and energy dissipation. A hard impact involving rigid surface has higher momentum transfer and less energy dissipation during impact. On the other hand, a soft impact provides increased energy dissipation due to the deformation of viscoelastic materials while momentum transfer is relatively decreased.
2. The numerical and experimental results show that a soft impact can reduce the vibration amplitude by 40 % compared with a hard impact. However, the difference in damping performance with tested viscoelastic materials is found to be minimum.
3. Integrating viscoelastic material resolves the common issues related with the SPID such as high-intensity impact force and noise levels. To observe the reduction in impact force, force sensors are installed at the walls if cavity in SPID. The results show a significant 96% reduction in impact force with a soft impact.
4. The experiments with soft and hard impacts are recorded and processed to determine the sound pressure levels (SPL). The results show that a SPID with soft impact does not generate any noise pollution during operation, while a SPID with hard impact increases the noise level by around 11.55dB during operation.

Compared with a multi-particle impact damper, a SPID is significantly easier to design, however, high-intensity impact force and noise were SPIDs major unresolved issues. These findings highlight the potential of viscoelastic materials in mitigating high-impact forces and noise levels in SPID, while improving the damping performance. Viscoelastic materials tested in this study are commercially available materials, therefore, an effective and safe SPID can be easily designed and installed. These results provide a basis for the SPID design and further advancements for optimal design and performance. Future studies can be conducted on analysing the damping performance of SPID with viscoelastic materials subject to several environmental conditions.

5. References

Akbar MA, Wong W-O and Rustighi E (2023) A Hybrid Damper with Tunable Particle Impact Damping and Coulomb Friction. *Machines* 11(5).

Akbar MA and Wong WO (2023) A Hybrid Damper with Particle Impact Damper and Coulomb Friction Designed for Free Vibration Damping. *Experimental Vibration Analysis for Civil Engineering Structures*. pp.550-559.

Akbar MA, Wong WO and Rustighi E (2024) Design optimization of a single-mass impact damper. *Journal Of Sound And Vibration* 570.

Araz O (2022) Optimization of three-element tuned mass damper based on minimization of the acceleration transfer function for seismically excited structures. *Journal of the Brazilian Society of Mechanical Sciences and Engineering* 44(10): 459.

Bai XM, Shah B, Keer LM, et al. (2009) Particle dynamics simulations of a piston-based particle damper. *Powder Technology* 189(1): 115-125.

Banerjee S, Ghosh A and Matsagar VA (2022) Optimum design of nonlinear tuned mass damper for dynamic response control under earthquake and wind excitations. *Structural Control and Health Monitoring* 29(7): e2960.

Chatterjee S, Mallik AK and Ghosh A (1995) On Impact Dampers for Non-Linear Vibrating Systems. *JOURNAL OF SOUND AND VIBRATION* 187(3): 403-420.

Djemal F, Chaari R, Gafsi W, et al. (2019) Passive vibration suppression using ball impact damper absorber. *Applied Acoustics* 147: 72-76.

Els DNJ (2011) Damping of Rotating Beams with Particle Dampers: Experimental Analysis. *Aiaa Journal* 49(10): 2228-2238.

Enríquez-Zárate J, Abundis-Fong HF, Velázquez R, et al. (2019) Passive vibration control in a civil structure: Experimental results. *Measurement and Control* 52(7-8): 938-946.

Gagnon L, Morandini M and Ghiringhelli GL (2019) A review of particle damping modeling and testing. *JOURNAL OF SOUND AND VIBRATION* 459: 114865.

Gao H, Wang C, Huang C, et al. (2020) Development of a Frequency-Adjustable Tuned Mass Damper (FATMD) for Structural Vibration Control. *SHOCK AND VIBRATION* 2020: 9605028.

Henriques IR, Rouleau L, Castello DA, et al. (2020) Viscoelastic behavior of polymeric foams: Experiments and modeling. *Mechanics of Materials* 148: 103506.

Housner GW, Bergman LA, Caughey TK, et al. (1997) Structural control: Past, present, and future. *Journal of Engineering Mechanics* 123(9): 897-971.

Huang XH, Li XJ and Wang J (2021) Optimal design of inerter-based nonpacked particle damper considering particle rolling. *EARTHQUAKE ENGINEERING & STRUCTURAL DYNAMICS* 50(7): 1908-1930.

Huang XH, Xu WB and Yan WM (2020) Equivalent model of a multiparticle damper considering the mass coupling coefficient. *STRUCTURAL CONTROL & HEALTH MONITORING* 27(8): e2580.

Jaisee S, Yue F and Ooi YH (2021) A state-of-the-art review on passive friction dampers and their applications. *Engineering Structures* 235: 112022.

Jami M, Rupakhety R, Bessason B, et al. (2024) Multimode Vibration Control Strategies of Long-Span Bridges Subjected to Multi-hazard: A Case Study of the Runyang Suspension Bridge. *Journal of Vibration Engineering & Technologies* 12(3): 4867-4880.

Kaul S (2021) Viscoelastic modeling—passive vibration isolators. *Modeling and Analysis of Passive Vibration Isolation Systems*. pp.27-61.

Koutsoloukas L, Nikitas N and Aristidou P (2022) Passive, semi-active, active and hybrid mass dampers: A literature review with associated applications on building-like structures. *Developments in the Built Environment* 12: 100094.

Li A (2020) Viscoelastic Damper. *Vibration Control for Building Structures*. Springer International Publishing, pp.129-160.

Li B, Dai K, Meng J, et al. (2021a) Simplified design procedure for nonconventional multiple tuned mass damper and experimental validation. *The Structural Design of Tall and Special Buildings* 30(2): e1818.

Li D, Tang H and Xue S (2021b) Robust design of tuned mass damper with hybrid uncertainty. *Structural Control and Health Monitoring* 28(10): e2803.

Lu Z, Lu X, Lu W, et al. (2012) Experimental studies of the effects of buffered particle dampers attached to a multi-degree-of-freedom system under dynamic loads. *JOURNAL OF SOUND AND VIBRATION* 331(9): 2007-2022.

Lu Z, Masri SF and Lu XL (2011) Parametric studies of the performance of particle dampers under harmonic excitation. *STRUCTURAL CONTROL & HEALTH MONITORING* 18(1): 79-98.

Lu Z, Wang ZX, Masri SF, et al. (2018) Particle impact dampers: Past, present, and future. *STRUCTURAL CONTROL & HEALTH MONITORING* 25: e2058.

Masri SF (1970) General Motion of Impact Dampers. *The Journal of the Acoustical Society of America* 47(1B): 229-237.

Masri SF and Caughey TK (1966) On the Stability of the Impact Damper. *Journal of Applied Mechanics* 33(3): 586-592.

Meador DJ and Mead DJ (1999) *Passive Vibration Control.* New York.

Meyer N and Seifried R (2020) Toward a design methodology for particle dampers by analyzing their energy dissipation. *Computational Particle Mechanics* 8(4): 681-699.

Momani L, Alsakarneh A, Tabaza TA, et al. (2021) Impact dynamics modelling of viscoelastic materials. *Materials Today-Proceedings* 38: 2968-2974.

Nehemy GF, Rustighi E, Gonçalves PJP, et al. (2023) A passive self-tuning vibration neutraliser using nonlinear coupling between the degrees of freedom. *Mechanical Systems and Signal Processing* 185: 109786.

Oyadiji SO (1996) Damping of vibrations of hollow beams using viscoelastic spheres. *Smart Structures and Materials 1996 Conference - Passive Damping and Isolation.* San Diego, California: Spie - Int Soc Optical Engineering, 89-98.

Prasad BB, Duvigneau F, Juhre D, et al. (2022) Damping performance of particle dampers with different granular materials and their mixtures. *Applied Acoustics* 200: 109059.

Rupakhety R, Elias S and Olafsson S (2020) Shared Tuned Mass Dampers for Mitigation of Seismic Pounding. *Applied Sciences* 10(6): 1918.

Safaeifar H and Sheikhi Azqandi M (2021) OPTIMAL DESIGN OF THE IMPACT DAMPER IN FREE VIBRATIONS OF SDOF SYSTEM USING ICACO. *International Journal of Optimization in Civil Engineering* 11(3): 461-479.

Salvi J, Rizzi E, Rustighi E, et al. (2018) Optimum Tuning of Passive Tuned Mass Dampers for the Mitigation of Pulse-Like Responses. *Journal of Vibration and Acoustics* 140(6).

Simonian S (2004) Particle Damping Applications. *45th AIAA/ASME/ASCE/AHS/ASC Structures, Structural Dynamics & Materials Conference*.

Sims ND, Amarasinghe A, Ridgway K, et al. (2005) Particle dampers for workpiece chatter mitigation. *ASME International Mechanical Engineering Congress and Exposition.* Orlando, FL: Amer Soc Mechanical Engineers, 825-832.

Snoun C and Trigui M (2018) Design parameters optimization of a particles impact damper. *International Journal of Interactive Design and Manufacturing - Ijidem* 12(4): 1283-1297.

Trigui M, Foltete E, Abbes MS, et al. (2009) An experimental study of a multi-particle impact damper. *Proceedings of the Institution of Mechanical Engineers Part C-Journal of Mechanical Engineering Science* 223(9): 2029-2038.

Trindade MA (2016) Passive and Active Structural Vibration Control. In: Lopes Junior V, Steffen Jr V and Savi MA (eds) *Dynamics of Smart Systems and Structures: Concepts and Applications*. Cham: Springer International Publishing, pp.65-92.

Wang BS, He HX, Chen YF, et al. (2022) Experimental and performance analysis of the combined damping system with a TMD and a multiple unidirectional single-particle damper. *JOURNAL OF SOUND AND VIBRATION* 540: 117301.

Wang L, Zhou Y and Shi W (2023) Seismic control of a smart structure with semiactive tuned mass damper and adaptive stiffness property. *Earthquake Engineering and Resilience* 2(1): 74-93.

Wang Q and Dan D (2022) A simplified modeling method for multi-particle damper: Validation and application in energy dissipation analysis. *JOURNAL OF SOUND AND VIBRATION* 517: 116528.

Wang Y, Lu Z and Du J (2020) Experimental study on damping mechanism of buffered impact dampers. *Applied Acoustics* 170: 107492.

Wei-ming Y, Bao-shun W and Hao-xiang H (2019) Research of mechanical model of particle damper with friction effect and its experimental verification. *JOURNAL OF SOUND AND VIBRATION* 460: 114898.

Wong C and Rongong J (2009) Control of Particle Damper Nonlinearity. *Aiaa Journal* 47(4): 953-960.

Wong WO, Fan RP and Cheng F (2018) Design optimization of a viscoelastic dynamic vibration absorber using a modified fixed-points theory. *The Journal of the Acoustical Society of America* 143(2): 1064-1075.

Xia Z, Liu X and Shan Y (2011) Application of particle damping for vibration attenuation in brake drum. *International Journal of Vehicle Noise and Vibration* 7(2): 178-194.

Yang YQ and Wang X (2019) Investigation into the linear velocity response of cantilever beam embedded with impact damper. *JOURNAL OF VIBRATION AND CONTROL* 25(7): 1365-1378.

Zhang Y, Cheng J, Xu W, et al. (2022) Particle Damping Vibration Absorber and Its Application in Underwater Ship. *Journal of Vibration Engineering & Technologies* 11(5): 2231-2248.

Zhou XQ, Yu DY, Shao XY, et al. (2016) Research and applications of viscoelastic vibration damping materials: A review. *Composite Structures* 136: 460-480.

Żurawski M, Graczykowski C and Zalewski R (2023) The prototype, mathematical model, sensitivity analysis and preliminary control strategy for Adaptive Tuned Particle Impact Damper. *JOURNAL OF SOUND AND VIBRATION* 564: 117799.